A.S. NIKOLENKO

V.E. Lashkaryov Institute of Semiconductor Physics, Nat. Acad. of Sci. of Ukraine
(45, Nauky Ave., Kyiv 03028, Ukraine; e-mail: nikolenko_ mail@ukr.net)

TEMPERATURE DEPENDENCE OF RAMAN SPECTRA OF SILICON NANOCRYSTALS IN OXIDE MATRIX

PACS 78.30.Am, 63.22.Kn

The temperature dependence of the Raman spectra of silicon nanocrystals (nc-Si) in a SiO_x matrix has been studied. The temperature evolution of the phonon spectra is considered as a result of the combined influence of the phonon-confinement effect, anharmonic phonon coupling, thermal expansion, and thermoelastic strains. The gradual relaxation of thermoelastic tensile strains in nc-Si with increase in the temperature is demonstrated. The effect of the laser heating on the Raman spectrum is studied, and the linear dependence of a local temperature in nc-Si on the power density of the exciting laser radiation is determined. The differences between the temperature dependences of the Raman spectra obtained at the thermal and local laser heatings of the nc-Si specimens are analyzed.

K e y w o r d s: silicon nanocrystallites, phonons, Raman microspectroscopy, laser heating.

1. Introduction

Silicon nanocrystals, when being located in materials with wider energy gaps, such as silicon oxides and nitrides, reveal quantum-mechanical properties at temperatures extending up to room one, which is promising for their application in silicon-based opto- and nano-electronics as light-emitting [1, 2], photodetecting [3], and photovoltaic elements [4]. The spatial confinement of charge carriers in silicon nanocrystallites (nc-Si) is responsible for the quantum-mechanical electronic properties of nc-Si and their dependence on the crystallite dimensions, shape, and environment [5,6]. The reduction of nc-Si dimensions to magnitudes comparable with the exciton Bohr radius gives rise to a growth of the nanocrystallite energy gap width, shift of the photoluminescence spectrum toward the visible range, and a substantial enhancement of the photoluminescence quantum efficiency [7].

Raman scattering spectroscopy (RSS) is a nondestructive express method for diagnosing the silicon nanostructures, which allows one to obtain information about their crystalline structure [8–11]. For single-crystalline silicon, the corresponding Raman spectra reveal a line near 521 cm^{-1} emerging due to the process of inelastic scattering by the triply degenerate optical vibration at the Brillouin zone center (T_{2g}). For nc-Si, the frequency position and the shape of the phonon band depend on the crystallite size, which is associated with the spatial phonon confinement effect. If the nc-Si dimensions are reduced to the nanoscale size, the vibration properties of silicon nanocrystallites become considerably modified due to the manifestation of the spatial phonon confinement effect. The phonon spectra of nanocrystallites are often analyzed in the framework of the model of strong spatial localization (confinement) of optical phonons, which was developed for the first time for spherical nc-Si [12] and extended further [13] onto nanocrystallites with various shapes. According to this model, the reduction of the nanocrystallite size to a value less than 10 nm results in the violation of selection rules for the wave vector ($q = 0$). Since the dispersion law for the TO-phonon branch has a decay character in a vicinity of the Γ point, the Raman spectrum demonstrates a low-frequency shift and an asymmetric broadening of the nc-Si phonon band with respect to that for single-crystalline Si. On the other hand, the effects of vibration anharmonicity and thermal expansion induced by the temperature growth in nc-Si – e.g., as a result of laser heating – also give rise to the low-frequency shift and broadening of the phonon band. This circumstance leads to an error while estimating the nanocrystallite size in the framework of the phonon confinement model [14]. In the present work, a somewhat different problem is put forward. To analyze the experimental Raman spectra of nanocrystalline silicon embedded into a di-

electric matrix with a wide energy gap with the use of the phonon confinement model, it is very important that temperature-dependent deformations that arise in the system as a result of the mismatch between the coefficients of thermal expansion in nanocrystallites, matrix, and substrate should be taken into account. It is so, because this procedure allows the error in the determination of nanocrystallite dimensions from nc-Si Raman spectra to be substantially reduced.

As a rule, the exciting laser radiation of about several milliwatts is focused in Raman microspectroscopy researches on an area several microns in diameter, which gives rise to high densities of the optical excitation power and stimulates the laser heating, i.e. the local temperature elevation in strongly absorbing materials [14]. In the case of nc-Si embedded into an oxide matrix, the effect of temperature growth induced by the laser heating is especially strong, because those nanocrystallites are characterized by a low thermal conductivity owing to the phonon scattering at their grain boundaries and structural defects. Moreover, the oxide matrix also possesses a low thermal conductivity (approximately several orders of magnitude lower in comparison with that in silicon single crystals) [14, 15]. This work is aimed at studying the combined action of the effects of strong spatial phonon localization, the temperature, laser heating, and thermoelastic strains on the Raman spectra of nc-Si in an oxide matrix in wide intervals of temperature and exciting radiation power.

2. Experimental Part

Films with silicon nanocrystallites in a SiO_x matrix are studied. The films were deposited onto quartz substrates, by simultaneously sputtering Si and SiO_2 targets in a magnetron, and then thermally annealed in an inert atmosphere at a temperature of 1400 K. The micro-Raman spectra were measured in the Stokes and anti-Stokes regions at room temperature in the inverse-scattering setup and with the help of a Horiba Jobin Yvon T64000 spectrometer equipped with an Olympus BX41 confocal microscope and a thermo-electrically cooled CCD detector. In order to measure the Stokes and anti-Stokes components in the Raman spectrum simultaneously, the triple mode of a spectrometer with subtraction of the dispersion was applied. The spectral resolution amounted to about 0.15 cm^{-1}. The Raman spectra
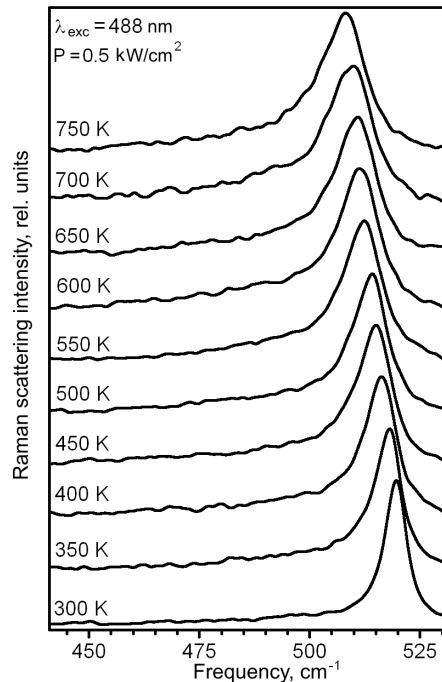

Fig. 1. Raman spectra of nc-Si measured at various specimen temperatures. $\lambda_{exc} = 488$ nm, $P = 0.5$ kW/cm^2

were excited using the line of an Ar–Kr laser with the wavelength $\lambda_{exc} = 488.0$ nm. Exciting radiation was focused on an area of about 5 μm^2 on the surface of a studied specimen with the help of an Olympus 10x/0.25 objective. The corresponding density of exciting radiation power on the specimen surface varied within the interval $P = 0.5 \div 100$ kW/cm^2. The specimen temperature in the measurement region was monitored, by using the ratio between the Stokes and anti-Stokes components in the nc-Si Raman spectrum. The temperature-dependent measurements of the nc-Si Raman spectra were carried out with the help of a thermo-electric cell Linkam THMS600 and varying the specimen temperature in the interval $T = 300 \div 750$ K.

3. Results and Their Discussion

3.1. Temperature dependence of nc-Si Raman spectra and thermoelastic strains

The temperature dependences of nc-Si Raman spectra were studied in the temperature interval of the thermally heated specimen from 300 to 750 K and at the exciting radiation power density of 0.5 kW/cm^2 (Fig. 1). In the nc-Si Raman spectra, a phonon band
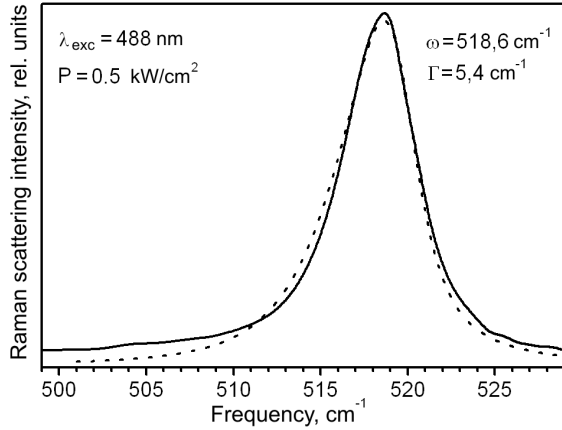
Fig. 2. Raman spectrum of nc-Si measured at room temperature and an excitation-radiation power density of 0.5 kW/cm². $\lambda_{\mathrm{exc}} = 488$ nm, $T = 300$ K

at about 520 cm^{-1}, which is connected with the process of inelastic scattering by LO-TO (T$_{2g}$) phonons in nc-Si, was registered.

Figure 2 exhibits the detailed shape of the Raman spectrum for nc-Si measured at room temperature. From this figure, one can see that the LO–TO phonon band of nc-Si at $\omega = 518.6$ cm^{-1} undergoes a low-frequency shift and a broadening ($\Gamma = 5.4$ cm^{-1}) with a strongly pronounced low-frequency asymmetry in comparison with that for Si single crystals, which is a characteristic attribute of the phonon Raman spectrum in nc-Si. Note that the broadening of the nc-Si LO–TO phonon band is associated with both the vibration anharmonicity enhancement in nanocrystallites, which results in a decrease of the optical phonon lifetime, and a dispersion of the nanocrystallite over sizes.

For spherical nc-Si of diameter L, we write down the phonon damping parameter in the form $\exp(-q^2 L^2/16\pi^2)$ and neglect the size dispersion of nanocrystallites. Then the intensity of the phonon band in the Raman spectrum can be expressed as follows in the framework of the model of strong phonon confinement [12, 13]:

$$I(\omega) = \int\limits_0^{2\pi/a} \frac{\exp(-q^2 L^2/16\pi^2)}{[\omega - \omega(q)]^2 + (\Gamma_0/2)^2} d^3q. \qquad (1)$$

Here, q is the wave vector, $a = 0.543$ nm is the lattice constant for silicon [16], $\omega(q)$ is the dispersion law for the phonon branch of TO vibrations (it can be

presented in the form $\omega^2(q) = A + B\cos(aq/4)$, where $A = 1.714 \times 10^5$ cm^{-2} and $B = 10^5$ cm^{-2}), and $\Gamma = 3.6$ cm^{-1} is the inherent halfwidth of the phonon band for single-crystalline silicon.

The fitting of the experimental nc-Si Raman spectrum (Fig. 2) by formula (1) allowed the average size of nc-Si to be determined: $L = 9$ nm. However, a shift of the nc-Si LO–TO phonon band by 1.3 cm^{-1} toward low frequencies in comparison with the theoretically calculated value was obtained. This additional low-frequency shift of the nc-Si phonon band can arise owing to tensile strains that emerge at the interfaces nc-Si/SiO$_x$ matrix and nc-Si/quartz substrate as a result of the different thermal expansion coefficients for heterostructure components [18]. In the case of biaxial elastic strains, the shift of the silicon phonon band is written down in the form [19, 20]

$$\Delta\omega(\sigma) = \frac{\sigma}{\omega_0}\left[(pS_{12} + q(S_{11} + S_{12})\right], \qquad (2)$$

where ω_0 is the LO–TO phonon band frequency in unstressed silicon, the elastic constants are $S_{11} = 7.68 \times 10^{-12}$ Pa^{-1} and $S_{12} = -2.14 \times 10^{-12}$ Pa^{-1}, and the phonon deformation potentials are $p = -1.43\omega_0^2$ and $q = -1.89\omega_0^2$ [20]. According to expression (2), the magnitude of tensile elastic strains that result in the low-frequency shift of the nc-Si phonon band $\Delta\omega = 1.1$ cm^{-1} equals 0.285 GPa.

As the temperature increases, the nc-Si phonon band gradually shifts toward low frequencies and broadens (Fig. 1). This temperature behavior of the phonon spectrum is typical of single-crystalline silicon and, as a rule, is associated with the anharmonic phonon–phonon interaction and the thermal expansion of the crystal as the temperature grows. The temperature dependence of the frequency shift of the nc-Si optical phonon band at the Brillouin zone center is described, in the general case, by the relation [21, 22]

$$\Delta\omega = \left[\frac{d\omega}{dT}\right]_V \Delta T + \left[\frac{d\omega}{dV}\right]_T \left[\frac{dV}{dT}\right]_P \Delta T =$$

$$= \Delta\omega_1(T) + \Delta\omega_2(T). \qquad (3)$$

The first term in expression (3) corresponds to the phonon band shift under the action of a phonon vibration anharmonicity at elevated temperatures. The effect of a phonon anharmonicity is well described

in a wide temperature interval if the anharmonic terms of the third and fourth orders are taken into cosideration. They describe the effect of the decay of long-wave optical phonons into low-frequency acoustic phonons in the course of three- and four-phonon scattering processes [23],

$$\Delta\omega_1(T) = A\left(1 + \frac{2}{e^x - 1}\right) +$$
$$+ B\left(1 + \frac{3}{e^y - 1} + \frac{3}{(e^y - 1)^2}\right), \qquad (4)$$

where $x = h\omega_0/2kT$, $y = h\omega_0/3kT$, and A and B are anharmonicity constants. Note that the anharmonicity of phonon vibrations must undoubtedly be taken into account at temperatures higher than the Debye one, T_D (for silicon, $T_D = 645$ K [24]), when all phonon vibrations are excited, and the further temperature elevation is accompanied by the growth of vibration amplitudes.

The second term, $\Delta\omega_2(T)$, in expression (3) describes the thermal expansion effect and, with regard for the Grüneisen parameter γ (for silicon, $\gamma = 0.98$ [25]), looks like [26]

$$\Delta\omega_2(T) = \omega_0\left(\exp\left(-3\gamma\int_0^T \alpha(T)dT\right) - 1\right), \qquad (5)$$

where ω_0 is the frequency of the phonon band location at $T = 0$ K, and $\alpha(T)$ is the temperature dependence of the thermal expansion coefficient. For silicon, the latter can be described by the empirical dependence [27]

$$\alpha(T) = (3.725(1 - \exp(-5.88 \times 10^{-3}(T - 124))) +$$
$$+ 5.548 \times 10^{-4}T) \times 10^{-6}(\text{K}^{-1}). \qquad (6)$$

In Fig. 3, the temperature dependence of the frequency position of the nc-Si phonon band is depicted, as well as the data of theoretical calculations carried out with regard for the anharmonicity of phonon vibrations and the thermally induced band broadening, $\Delta\omega_1 + \Delta\omega_2$ (dash-dotted curve) and using the coefficients of anharmonicity for single-crystalline silicon ($A = -3.45$ cm^{-1} and $B = -0.050$ cm^{-1} [28]) and the coefficient of thermal expansion in the form (6). Additionally, Fig. 3 shows the contributions of the anharmonic interaction, $\Delta\omega_1$ (dotted curve), and
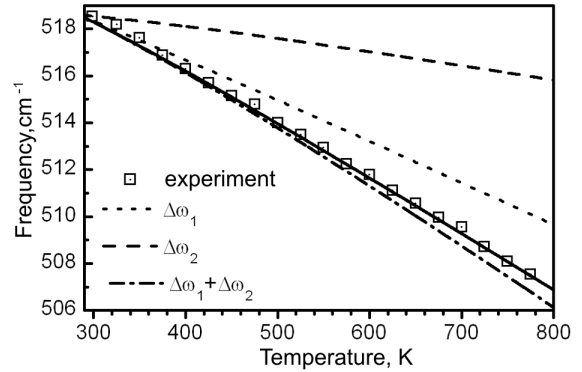

Fig. 3. Temperature dependence of the frequency position of the nc-Si LO–TO phonon band (solid curve), the contributions associated with the anharmonicity of phonon vibrations $\Delta\omega_1$ (dotted curve) and the thermal expansion $\Delta\omega_2$ (dashed curve), and the result of calculation making allowance for both mechanisms $\Delta\omega_1 + \Delta\omega_2$ and the results of work [28] (dash-dotted curve)

thermal expansion, $\Delta\omega_2$ (dashed curve), separately. One can see that the curve theoretically calculated making allowance for both contributions, $\Delta\omega_1 + \Delta\omega_2$, agrees well with the experimental data obtained at room temperature. As the temperature grows, a gradual shift of the calculated curve into the low-frequency region is observed. The approximation of experimental data by expression (3) brought about the anharmonicity coefficient values $A = -3.44$ cm^{-1} and $B = -0.0015$ cm^{-1}. The coefficient A is close to the corresponding value for single-crystalline silicon, whereas the value of coefficient B is much smaller than its counterpart. The latter circumstance can be associated with the fact that, when fitting the experimental data, the above-mentioned temperature dependence of tensile strains in nc-Si was not taken into account. The difference between the temperature dependences of the thermal expansion coefficients for the nc-Si film, matrix, and quartz substrate can give rise to thermally induced strain changes in the examined heterosystem. Since elastic strains in the analyzed system "nc-Si in an oxide matrix" can substantially depend on the mismatch between the coefficients of thermal expansion in the nc-Si, SiO$_x$ matrix, and quartz substrate, the calculation of the contribution made by temperature-dependent elastic strains is a rather complicated problem. However, in our case, thermoelastic strains can be estimated from the difference between the experimental temperature de-
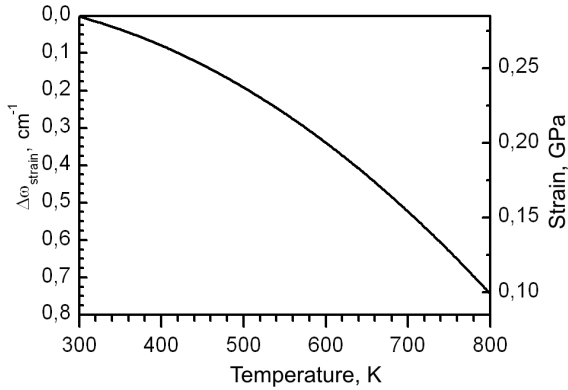
Fig. 4. Temperature dependence of the frequency shift of the nc-Si LO–TO phonon band stimulated by thermoelastic strains, $\Delta\omega_{\mathrm{strain}}$, and estimation of a strain magnitude

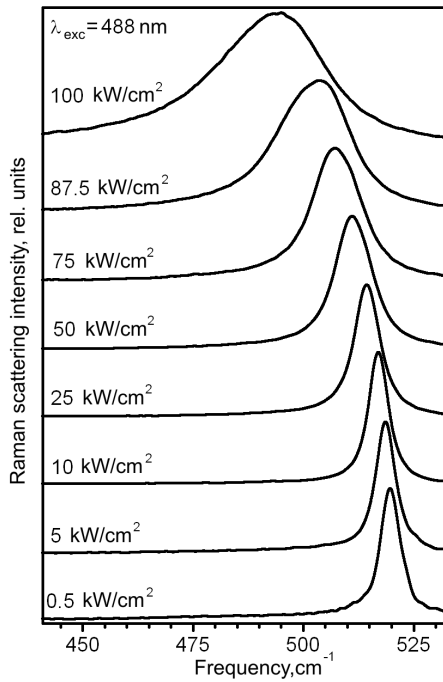**Fig. 5.** Raman spectra of nc-Si measured at various laser excitation power densities. $\lambda_{\mathrm{exc}} = 488$ nm

pendence of the phonon band frequency (solid curve in Fig. 3) and the theoretically calculated one taking the contributions of anharmonicity and thermal expansion (dash-dotted curve in Fig. 3) into account. In Fig. 4, the calculated temperature dependence of the nc-Si phonon band frequency shift associated with thermoelastic strains in the examined heterosystem, $\Delta\omega_{\mathrm{strain}}$, is depicted, and the magnitudes of those

strains are estimated in accordance with expression (2). One can see that the temperature growth is accompanied by a gradual relaxation of tensile strains in nc-Si. This result is reasonable because the strains concerned stem from the discrepancy between the thermal expansion coefficients of the structure components when the structure is cooled down after its thermal annealing at $T = 1400$ K.

3.2. Laser heating effect

To study the laser heating effect in nc-Si, the nc-Si Raman spectra were measured for various densities of exciting radiation power within the interval 0.5–100 kW/cm^2 (Fig. 5). When this parameter grows, a gradual low-frequency shift and a broadening of the nc-Si phonon band were observed, which can be associated with the growth of the local temperature owing to the heating of nanocrystallites by laser radiation.

The temperature of studied nanocrystallites is estimated from the following relation between the integral intensities of Stokes and anti-Stokes components in the nc-Si Raman spectrum [29]:

$$\frac{I_{\mathrm{S}}}{I_{\mathrm{AS}}} = C \left(\frac{\omega_l + \omega_{\mathrm{S}}(T)}{\omega_l - \omega_{\mathrm{S}}(T)}\right)^4 \exp\left(\frac{\hbar\omega_{\mathrm{S}}(T)}{kT}\right), \qquad (7)$$

where ω_l, ω_{S}, and ω_{AS} are the frequencies of exciting laser radiation, and the Stokes and anti-Stokes components in the nc-Si phonon Raman spectrum, respectively. The coefficient C depends on experimental conditions and is governed by the efficiency of light scattering and the experimental conditions of Raman spectrum registration in the Stokes and anti-Stokes ranges (such as the light absorption coefficients, scattering cross-sections, resonance conditions, spectral sensitivity, and so forth). This coefficient was determined from the ratio between the Stokes and anti-Stokes component intensities in the nc-Si Raman spectrum measured under the given experimental conditions and at the thermal heating of the examined specimen. In order to determine the coefficient C numerically, it is convenient to rewrite expression (7) in the form of the logarithmic dependence of the ratio $I_{\mathrm{S}}/I_{\mathrm{AS}}$ on the reciprocal temperature, namely,

$$\ln\frac{I_{\mathrm{S}}}{I_{\mathrm{AS}}} = \ln(C) + 4\ln\left(\frac{\omega_l + \omega_{\mathrm{S}}(T)}{\omega_l - \omega_{\mathrm{S}}(T)}\right) + \frac{1}{T}\frac{\hbar\omega_{\mathrm{S}}(T)}{k}. \quad (8)$$

The approximation of experimental data (Fig. 6) obtained at the thermal heating of the specimen (Fig. 1),

which was made using expression (8), gave the value $C = 0.875$.

In Fig. 7, the dependence of the local temperature in nc-Si on the density of exciting laser radiation power is depicted. The temperature values were determined from expression (7) describing the ratio between the intensities of Stokes and anti-Stokes components in the nc-Si Raman spectrum, in which the value of the coefficient C quoted above was used. From Fig. 7, one can see that a growth of the excitation power density to 100 kW/cm^2 results in a linear growth of the local temperature in the studied nc-Si from room temperature to 850 K at a rate of 5.12 K×cm^2/kW. The obtained value of local temperature in nc-Si turned out rather high at relatively low intensities of laser excitation, which can be associated with the low thermal conductivities of heterosystem's components (nc-Si in the oxide matrix). More specifically, these are the low thermal conductivity of the SiO$_x$ matrix (at room temperature, the thermal conductivity of SiO$_2$ amounts to 1.4 W/(m×K) in contrast to a value of 156 W/(m×K) for bulk Si [30]) and a decrease of the thermal conductivity of the system owing to the phonon scattering at nanocrystallite boundaries, interfaces, and structural defects [14, 15]. It should also be noted that, at the excitation power densities $P \leq 5$ kW/cm^2, the influence of the laser heating effect in nc-Si is insignificant.

In Fig. 8, the temperature dependence of the LO–TO phonon band frequency in nc-Si at its laser heating is exhibited. For the sake of comparison, the results obtained at the direct heating of a specimen are also presented. One can see that the temperature growth induced by the laser heating gives rise to a gradual frequency shift of the nc-Si phonon band into the low-frequency range that is larger in comparison with the shift obtained at the direct heating. At temperatures $T > 750$ K, the phonon band shifts toward lower frequencies much more strongly.

One of the reasons why the observed difference between the rates of frequency changes at temperatures below and above 750 K may originate from different characters of thermoelastic strains. In particular, if the local laser heating is applied to an nc-Si film, the macroscopic deformations stemming from the inequality of the thermal expansion coefficients in the quartz substrate and nc-Si do not relax.

A considerable low-frequency shift of the phonon band (up to 494 cm^{-1}) at a low temperature
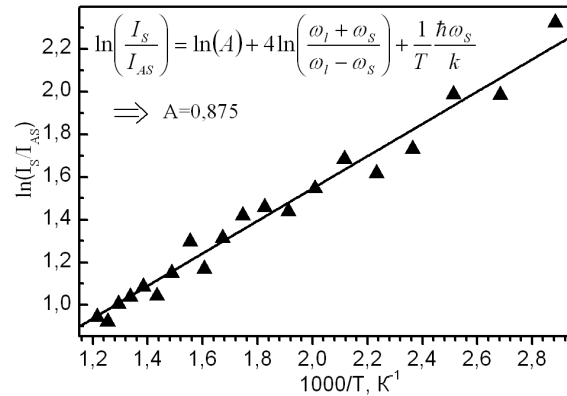

$$\ln\left(\frac{I_S}{I_{AS}}\right) = \ln(A) + 4\ln\left(\frac{\omega_l + \omega_S}{\omega_l - \omega_S}\right) + \frac{1}{T}\frac{\hbar\omega_S}{k}$$

$$\Rightarrow A = 0,875$$

Fig. 6. Dependence of the intensity ratio between the Stokes and anti-Stokes components in the nc-Si Raman spectrum on the temperature
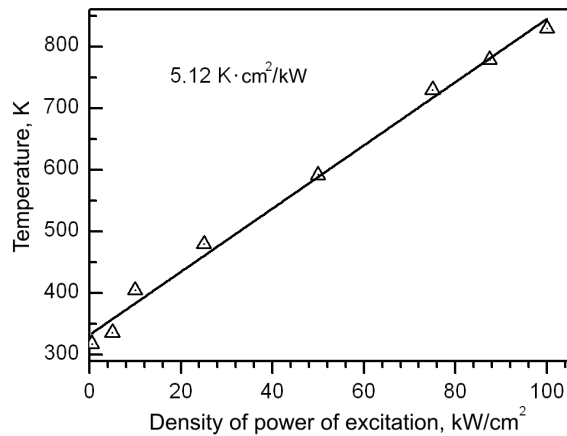

Fig. 7. Dependence of the nc-Si temperature on the density of exciting laser radiation power
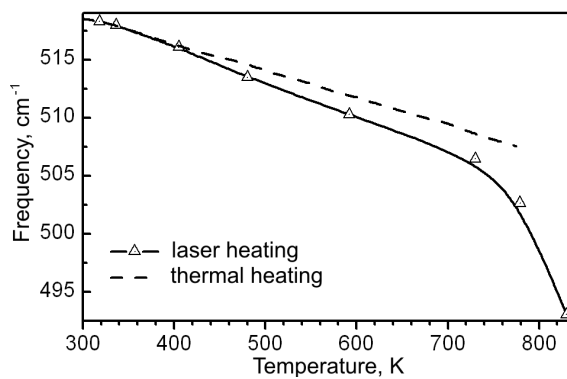

Fig. 8. Temperature dependences of the frequency position of the nc-Si LO–TO phonon band obtained at the direct heating of the studied structure (dashed curve) and at the laser heating in the course of measurement (solid curve)

($T = 830$ K) is unusual. For comparison, the same shift in single-crystalline silicon is observed at temperatures of about 1200 K [23]. This effect can be explained only if additional physical mechanisms giving rise to a modification of the nc-Si phonon spectra and becoming active at high exciting radiation power densities are supposed to take place. An enhancement of the anharmonic interaction between phonons owing to a strong excitation of the phonon subsystem in nc-Si can be one of them. In this case, the anharmonic phonon–phonon interaction can result in additional violations of selection rules with respect to the wave vector and to the involvement of phonons with nonzero wave vectors into light scattering processes, which leads to an extra low-frequency shift of the nc-Si phonon band. The anharmonicity of low-frequency acoustic phonons [11] and surface phonon modes [15] can be another channel of the optical phonon damping. In addition, at high exciting radiation powers, the probability for the Fano resonance between optical phonons and the continuum of states of photo-induced charge carriers to manifest itself grows [31, 32]. A more detailed analysis of this unusual temperature behavior of the nc-Si phonon band needs to be researched further.

4. Conclusions

In this work, the temperature dependence of the Raman spectra for silicon nanocrystallites is studied. It is shown that the temperature-induced low-frequency shift of the nc-Si phonon band is caused by a combined action of such phenomena as the spatial confinement of phonons, the anharmonic interaction between them, and thermoelastic strains. The character of the temperature dependence of thermoelastic strains is established. The low-frequency shift and the broadening of the nc-Si phonon band observed as the density of laser excitation power grows is connected with the laser heating effect. The linear dependence of the attained nc-Si temperature on the laser excitation power density is obtained with a proportionality coefficient of 5.12 K·cm^2/kW. The discrepancy between the temperature dependences of the nc-Si phonon band frequency at the thermal and local laser heatings of the specimen in the temperature interval $T < 750$ K is explained by different characters of thermoelastic strains. The substantial low-frequency shift of the nc-Si phonon band

at temperatures $T > 750$ K can result from the influence of other physical mechanisms of phonon scattering that manifest themselves at high densities of laser excitation power (the enhancement of the phonon anharmonicity and the violation of selection rules at Raman scattering, the anharmonicity of low-frequency acoustic phonons, and the Fano resonance).

1. R. Collins, P.M. Fauchet, and M.A. Tischler, Phys. Today **50**, No. 1, 24 (1997).
2. K.D. Hirschman, L. Tsybeskov, S.P. Duttagupta, and P.M. Fauchet, Nature **384**, 338 (1996).
3. Z. Huang, J.E. Carey, M. Liu, X. Guo, E. Mazur, and J.C. Campbell, Appl. Phys. Lett. **89**, 033506 (2006).
4. S. Park, E. Cho, D. Song, G. Conibeer, and M.A. Green, Sol. Energy Mater. Sol. Cells **93**, 684 (2009).
5. M.N. Islam and S. Kumar, J. Appl. Phys. **93**, 1753 (2003).
6. X.X. Wang, J.G. Zhang, L. Ding, B.W. Cheng, W.K. Ge, J.Z. Yu, and Q.M. Wang, Phys. Rev. B **72**, 195313 (2005).
7. M.V. Wolkin, J. Jorne, P.M. Fauchet, G. Allan, and C. Delerue, Phys. Rev. Lett. **82**, 197 (1999).
8. A.S. Nikolenko, M.V. Sopinskyy, V.V. Strelchuk, L.I. Veligura, and V.V. Gomonovych, J. Optoelectron. Adv. Mater. **14**, 120 (2012).
9. S. Hernandez, A. Martinez, P. Pellegrino, Y. Lebour, B. Garrido, E. Jordana, and J.M. Fedeli, J. Appl. Phys. **104**, 044304 (2008).
10. T. Arguirov, T. Mchedlidze, M. Kittler, R. Rolver, B. Berghoff, M. Forst, and B. Spangenberg, Appl. Phys. Lett. **89**, 053111 (2006).
11. G. Viera, S. Huet, and L. Boufendi, J. Appl. Phys. **90**, 4175 (2001).
12. H. Richter, Z.P. Wang, and L. Ley, Solid State Commun. **39**, 625 (1981).
13. I.H. Campbel and P.M. Fauchet, Solid State Commun. **58**, 739 (1984).
14. V. Poborchii, T. Tada, and T. Kanayama, J. Appl. Phys. **97**, 104323 (2005).
15. G. Faraci, S. Gibilisco, and A.R. Pennisi, Phys. Lett. A **373**, 3779 (2009).

986

16. M.E. Straumanis and E.Z. Aka, J. Appl. Phys. **23**, 330 (1952).

17. M. Salis, P.C.Ricci, and A.Anedda, J. Raman Spectrosc. **40**, 64 (2009).

18. G. Lucovsky and J.C. Phillips, J. Vac. Sci. Technol. B **22**, 2087 (2004).

19. I. De Wolf, Semicond. Sci. Technol. **11**, 139 (1996).

20. E. Anastassakis, A. Pinczuk, E. Burstein, F.H. Pollak, and M. Cardona, Solid State Commun. **8**, 133 (1970).

21. C. Postmus, J.R. Ferraro, and S.S. Mitra, Phys. Rev. **174**, 983 (1968).

22. E.S. Zouboulis and M. Grimsditch, Phys. Rev. B **43**, 12490 (1991).

23. M. Balkanski, R.F. Wallis, and E. Haro, Phys. Rev. B **28**, 1928 (1983).

24. R. Hull, *Properties of Crystalline Silicon* (INSPEC, Institute of Electrical Engineers, London, 1999).

25. B.A. Weinstein and G.J. Piermarini, Phys. Rev. B **12**, 1172 (1975).

26. W.J. Borer, S.S. Mitra, and K.V. Namjoshi, Sol. State Commun. **9**, 1377 (1971).

27. Y. Okada and Y. Tokumara, J. Appl. Phys. **56**, 314 (1984).

28. H. Tang and I.P. Herman, Phys. Rev. B **43**, 2299 (1991).

29. T.R. Hart, R.L. Aggarwal, and B. Lax, Phys. Rev. B **1**, 638 (1970).

30. S.M. Sze, *Physics of Semiconductor Devices* (Wiley, New York, 1981).

31. A.K. Shukla, R. Kumar, and V. Kumar, J. Appl. Phys. **107**, 014306 (2010).

32. R. Gupta, Q. Xiong, C.K. Adu, U.J. Kim, and P.C. Eklund, Nano Lett. **3**, 627 (2003).

А.С. Ніколенко

ТЕМПЕРАТУРНА ЗАЛЕЖНІСТЬ
СПЕКТРІВ КОМБІНАЦІЙНОГО РОЗСІЯННЯ
СВІТЛА КРЕМНІЄВИХ НАНОКРИСТАЛІТІВ
В ОКСИДНІЙ МАТРИЦІ

Р е з ю м е

Досліджено температурну залежність спектрів комбінаційного розсіяння світла (КРС) кремнієвих нанокристалітів (nc-Si) в матриці SiO_x. Зміну фононного спектра з температурою проаналізовано з врахуванням комбінованого впливу ефектів просторового обмеження фононів, ангармонічної взаємодії, термічного розширення та термопружних деформацій. Показано поступову релаксацію термопружних деформацій розтягу nc-Si при зростанні температури. Досліджено вплив ефекту лазерного розігріву на фононний спектр nc-Si та встановлено лінійну залежність локальної температури nc-Si від густини потужності збуджуючого лазерного випромінювання. Проаналізовано відмінності температурних залежностей спектрів КРС nc-Si при термічному нагріванні зразка та локальному лазерному розігріві.